Receive Beamforming for Ultrareliable Random Access based SWIPT

S. Kisseleff, S. Chatzinotas, and B. Ottersten
Interdisciplinary Centre for Security, Reliability and Trust (SnT),
University of Luxembourg, Luxembourg.

***Abstract*—Ultrareliable unscheduled communication using short packets poses novel research challenges for the receiver design. Here, the uncertainty imposed by the random access and a large amount of interfering transmissions is the limiting factor for the system performance. Recently, this type of communication has been addressed in context of simultaneous wireless information and power transfer (SWIPT). The need to adapt the power splitting to the signal states according to the underlying random access has been tackled by introducing a predictor, which determines the valid states of the received signal based on the long-term observation. Hence, the power splitting factor is scaled accordingly in order to guarantee ultrareliable communication and maximized harvested energy.**
In this work, we extend the considered SWIPT scenario by introducing multiple antennas at the receiver side. Through this, the received energy can be substantially increased, if the energy harvesting parameters and the spatial filter coefficients are jointly optimized. Hence, we propose an optimization procedure, which aims at maximizing the harvested energy under the ultrareliability constraint. The mentioned prediction methods are combined with the optimization solution and the resulting system performance is numerically evaluated.

I. Introduction

Co-channel interference from simultaneous transmissions is one of the main challenges for the design of large communication networks, such as Internet-of-Things (IoT) or Low Power Wide Area Networks (LPWANs) [1]. Typically, the interfering transmissions are separated via orthogonal multiple access (OMA) techniques in time, frequency, code or spatial domain. However, the resulting network throughput reduces with increasing number of network nodes. In addition, the packet duration may reach very high values, which might be very crucial for various aspects of system performance, e.g. latency, network stability, etc. In order to adapt to the low throughput of the OMA, the duty cycle of each node needs to be increased as well. Alternatively, a non-orthogonal multiple access (NOMA) can be applied in order to accommodate multiple data streams in one transmission channel, cf. [2]. However, these data streams need to be sufficiently separable, e.g. in terms of signal power. This separability is usually limited to only a few parallel data streams. Another solution is based on random medium access (RMA), which utilizes unscheduled transmissions from multiple nodes and is known to have a lower bound for the network throughput, e.g. the well-known lower bounds of the ALOHA protocols. Unlike OMA and NOMA, RMA introduces an additional uncertainty in terms of packet arrival probability. This uncertainty can be sometimes exploited in order to improve the reliability of information decoding, cf. [3]. Furthermore, RMA provides a substantial flexibility for the design of large communication networks, since no scheduling is required, which simplifies the integration of new nodes into the network.

In order to realize RMA, short data packets are transmitted from each node according to the underlying random process. The discontinuous transmission of short packet has recently gained attention in the context of ultrareliable low-latency communication, where extremely low symbol error probabilities are the main requirement and challenge [4]. In this context, the resource allocation and the accuracy of channel estimation under the assumed constraints of ultra-reliability and ultra-low latency are of major interest, cf. [5]. Furthermore, various scenarios have been investigated, e.g. relaying based transmissions [6], and multiple-input multiple-output (MIMO) systems [7]. However, all these works pose hard constraints on the scheduling of transmissions, which render the proposed methods not applicable to RMA. On the other hand, a combination of unscheduled short packet transmissions and simultaneous wireless information and power transfer (SWIPT) has been addressed in [8].

Similarly to [8], we consider a relay-aided single cluster uplink of a large network, e.g. IoT. Here, the nodes of the same cluster transmit their data to the relay, which acts as a cluster head, processes the received data by means of redundancy reduction, and forwards it to the base station. Furthermore, the relay transmissions can be event-driven, such that the data is only forwarded to the base station, if it is sufficiently novel and spatially diverse. Correspondingly, the amount of data to be transmitted and the resulting power consumption at the relay are low, such that the relay can be even wirelessly powered via energy harvesting[1]. Furthermore, the data and the energy need to be received at the same time, which suggests the use of SWIPT [9]. In [8], the basic design guidelines have been proposed for a multiple access single-input single-output (SISO) scenario. In particular, the necessity of prediction of the symbol constellation and the optimization of the dynamically adjustable power splitting factor has been explained. In this work, we extend the considered system to a multiple access single-input multiple-output (SIMO) scenario by introducing multiple receive antennas at the relay. In general, joint receive beamforming and energy harvesting as

This work was supported by the Luxembourg National Research Fund (FNR) in the framework of the FNR-FNRS project "InWIP-NET : Integrated Wireless Information and Power Networks".

[1]We assume, that the nodes are not too far away from the relay in order to enable the energy harvesting.

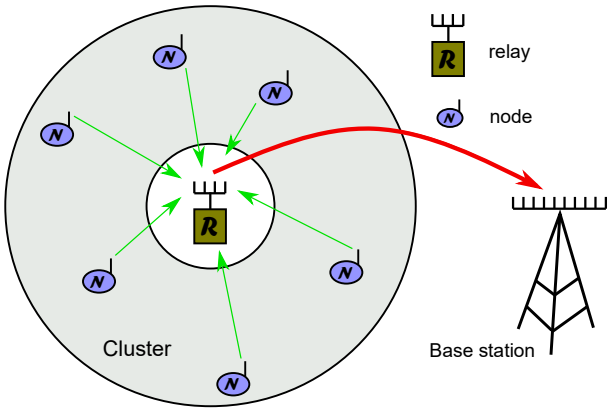

Fig. 1. IoT cluster with a SWIPT-enabled relay.

an optimization problem has rarely been addressed so far. In [10], the authors assume a single transmitter and deduce the beamforming coefficients from the normalized channel vector. Furthermore, the receive beamforming has been optimized for a constant power splitting factor in [11]. However, a joint maximization of the harvested energy under the ultrareliability constraint is necessary for the considered scenario and is proposed here for the first time.

This paper is organized as follows. In Section II, we describe the employed system model based on the randomly scheduled ultrareliable SWIPT for a wireless powered relay. Based on the system model, we formulate the optimization problem in Section III. This problem is then solved by splitting it in two sub-problems, which are solved alternatingly. In Section IV, the performance of the proposed method is evaluated. Subsequently, the paper is concluded in Section V.

II. System Model

A. Notation

Throughout the paper, we denote $(\cdot)^T$ and $(\cdot)^H$ the transpose and Hermitian transpose operations, respectively. Complex conjugation is denoted by $(\cdot)^*$. The expression $\mathbf{x} \prec y$ indicates that each element of $\mathbf{x}$ is smaller than y. Furthermore, $diag(\mathbf{x})$ denotes a diagonal matrix with elements of vector $\mathbf{x}$ on its main diagonal. In addition, $\mathbf{0}$ denotes an all-zero column vector and $\mathbf{I}$ represents the unity matrix. The notation $vec(x, K) = [x_1, x_2, \ldots, x_K]^T$ is introduced in order to avoid repeating similar definitions of the signal vectors. Also, we denote $Q(\cdot)$ and $Q^{-1}(\cdot)$ the complementary Gaussian error integral and its inverse, respectively. $\mathcal{E}\{\cdot\}$ represents the expectation operator with respect to the symbol intervals.

B. Scenario

We assume a stationary deployment of N IoT nodes in close proximity of the energy-harvesting relay. The relay detects the symbols of transmitted data packets from all nodes, processes the data, and forwards it to the destination. The network structure is depicted in Fig. 1.

We assume a perfect channel state information (CSI) and synchronization between each node and the relay. However, individual duty cycles and scheduling of transmissions are unknown at the relay. Furthermore, each node n may transmit the respective data packets of length L_n with probability p_n, such that the transmissions from different nodes may overlap in time, which typically results in a joint symbol constellation observed at the relay.

Each node is equipped with a single transmit antenna, whereas the relay has K receive antennas. The diversity of the receive antennas can be exploited e.g. in order to increase the detection reliability or the network throughput. In this work, we focus solely on the single receive beamformer design for power gain, i.e. we do not exploit the spatial domain in order to decouple the data streams via spatial demultiplexing, which would require the design of multiple beamformers.

C. Signal transmission

The data packets are modulated via binary phase-shift keying (BPSK) in order to account for the typically low-power and low-complexity transceivers utilized as IoT nodes. This yields a sequence of symbols $c_{n,k}[m] \in \{-1, +1\}$, $1 \leq m \leq L_n$ for each packet l transmitted by node n in symbol interval m of length T. Typically, the data is protected via forward error correction (FEC), which introduces some dependencies among the individual symbols of the packet. These dependencies are related to the applied channel code and transmitted data. Due to the frequent overlaps of multiple packets, these dependencies can hardly be exploited [8]. For simplicity, we assume that the a-priori probabilities of the transmit symbols are unknown to the receiver.

In order to model the RMA based packet transmission, we introduce a discrete random variable $\mu_{n,l}$, which describes the spacing between packet $l-1$ and l of node n. Here, the probability for $\mu_{n,l}$ empty symbol intervals between two packets is given by

$$\Pr(\mu_{n,l}) = p_n(1-p_n)^{\mu_{n,l}}. \tag{1}$$

Hence, the total sequence of symbols $a_n[m]$ transmitted by node n is obtained via summation of all time-shifted packets:

$$a_n[m] = \sum_{l=-\infty}^{\infty} c_{n,l}[m - ((l-1)L_n + \mu_{n,l})]. \tag{2}$$

Assuming an equal transmit power P_t for all nodes during packet transmission, the average consumed power is (cf. [8])

$$P_{\text{trans},n} = P_t \frac{p_n L_n}{p_n L_n + (1-p_n)}, \tag{3}$$

since L_n symbols are transmitted with probability of p_n (the respective consumed power is $P_t p_n L_n$) and 1 symbol interval remains empty with probability of $1-p_n$ (the respective consumed power is 0). Note, that we do not take into account the energy consumption related to signal processing at the relay, which might need to be considered in the future extensions of our work.

We assume a frequency-flat quasi-static block fading channel with the complex-valued channel vector $\mathbf{h}_n = vec(h_n, K)$ between the transmit antenna of node n and the relay receive antennas. The overall channel matrix between all nodes and the relay is denoted as $\mathbf{H} = [\mathbf{h}_1, \mathbf{h}_2, \ldots, \mathbf{h}_N] \in \mathcal{C}^{K \times N}$.

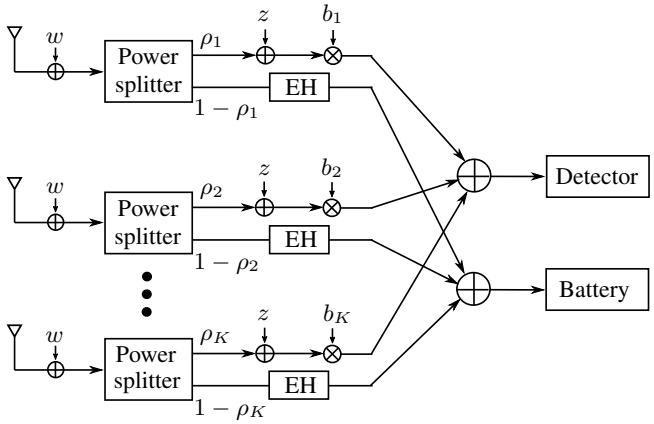

Fig. 2. Power splitting at the receiver equipped with multiple antennas.

D. Energy harvesting and signal detection

The two major methods for energy harvesting in SWIPT are time splitting (TS) and power splitting (PS), cf. [12]. As discussed in [8], the TS method of SWIPT is not applicable in the considered scenario, since some of the nodes may start their transmissions during the energy harvesting phase. Correspondingly, parts of the transmitted packets might be lost, which violates the assumed ultrareliability of symbol detection. Hence, the PS method is selected for the SWIPT. Moreover, we utilize dynamically adjustable PS factors similar to [13], which can be modified in each symbol interval. Furthermore, a symbol-by-symbol joint detection (JD) of multiple streams has been suggested instead of a successive interference cancellation (SIC). Although SIC is commonly used for the separation of data streams in NOMA [2], the adaptation of the PS factor cannot wait for the reception of the whole packet in order to exploit the dependencies among symbols. Hence, JD is selected as signal detection method.

In this work, we utilize multiple PS modules, which are connected to the respective antennas. The basic structure of the SWIPT-enabled receiver with multiple antennas is similar to [13] and is depicted in Fig. 2. Here, the received signal from each antenna k is at first fed into the respective power splitter with the PS factor $\rho_k[m]$ in symbol interval m. At the output of the power splitter, one signal is used for information detection and the other for energy harvesting. The spatial filtering is applied after the power splitting by multiplying the data carrying signal part with the respective complex-valued beamforming coefficient $b_k[m]$. This architecture ensures that it is possible to exploit the spatial diversity of the communication channel, since the summation of the signals is done after the power splitting. If the summation was applied before the PS, it would not be possible to use the receive beamforming without injecting additional power into the system[2]. On the other hand, the use of multiple energy harvesting modules (EHs) guarantees that the maximum energy is harvested in each symbol interval, since the destructive overlap of the energy signals is avoided.

After the spatial filtering, the signal is fed into the information detector[3]. The signal at the input of the symbol detector is given by

$$r[m] = \sqrt{P_t}\mathbf{b}^H[m]\mathbf{S}[m]\left(\mathbf{H}\mathbf{a}[m] + \mathbf{w}[m]\right) + \mathbf{b}^H[m]\mathbf{z}[m], \quad (4)$$

where $\mathbf{b}[m] = vec(b^*[m], K)$, $\mathbf{a}[m] = vec(a[m], N)$. Also, $\mathbf{w}[m] = vec(w[m], K)$ is the sampled received noise vector with the known variance $\mathcal{E}\{|w_k[m]|^2\} = \sigma^2$, $\forall k$. Note, that the power splitter imposes additional noise for the information detection, which is modeled via an additive white Gaussian noise signal $z_k[m]$ with the variance $\mathcal{E}\{|z_k[m]|^2\} = \delta^2$, $\forall k$, similar to [12]. We stack the individual noise contributions into vector $\mathbf{z}[m] = vec(z[m], K)$. The impact of the power splitting is taken into account in the matrix $\mathbf{S}[m] = diag(vec(\sqrt{\rho[m]}, K))$.

Obviously, the symbol constellation observed at the receiver is a combination of distorted individual symbol constellations of all active nodes (assuming a perfect synchronization of frequency and time). Due to the random process of packet generation, the number of points in this joint constellation varies from symbol interval to symbol interval between 1 and 2^N depending on the number of active nodes. Correspondingly, the signal quality varies as well. The instantaneous signal quality of the received signal in terms of signal-to-noise ratio (SNR) can be formulated as follows:

$$\mathrm{SNR}[m] = \frac{P_t \left|\mathbf{b}^H[m]\mathbf{S}[m]\mathbf{H}\mathbf{a}[m]\right|^2}{\delta^2\mathbf{b}^H[m]\mathbf{b}[m] + \sigma^2\mathbf{b}^H[m]\mathbf{S}[m]\mathbf{S}[m]\mathbf{b}[m]}. \quad (5)$$

Unfortunately, the a-priori probability of each symbol in the individual symbol constellations and therefore in the joint symbol constellation is unknown, as mentioned earlier. Hence, the symbolwise a-posteriori detection is not possible in this case. Instead, we implicitly utilize the maximum-likelihood criterion for the symbol detection by assuming that all points of the joint constellation are equally probable.

As argued in [8], in order to achieve ultrareliable communication, we base our investigation upon a conservative upper bound on the symbol error rate related to the probability of error between the closest points of the joint symbol constellation. This strategy is sometimes used in multiuser detection scenarios [14]. For this, we define a metric $d_{i,j}[m]$, which corresponds to the Euclidean distance between the points with indices i and j of the joint constellation. In addition, we introduce vectors $\mathbf{q}_i[m]$ and $\mathbf{q}_j[m]$ of length N, which pertain to these points. These vectors contain the respective combinations of symbols transmitted by individual nodes in symbol interval m (including empty symbol intervals in case of inactive nodes), e.g. $\mathbf{q}_i[m] = [-1, 0, +1, -1]^T$. Correspondingly, $d_{i,j}[m]$ is obtained via

$$d_{i,j}[m] = \sqrt{P_t}\left|\mathbf{b}^H[m]\mathbf{S}[m]\mathbf{H}\left(\mathbf{q}_i[m] - \mathbf{q}_j[m]\right)\right|. \quad (6)$$

Using $d_{i,j}[m]$, it is possible to determine the upper bound of the symbol error rate by calculating a modified SNR based on the minimum distance between the valid points of the joint

[2]In practice, signal multiplication implies an additional power consumption in the circuits, which might be even larger than the received power.

[3]Typically, matched filtering and sampling are applied here prior to symbol detection.

constellation:

$$\mathrm{SNR}_{\mathrm{mod}}[m] = \frac{\left|\frac{1}{2}\min_{i,j} d_{i,j}[m]\right|^2}{\delta^2 \mathbf{b}^H[m]\mathbf{b}[m] + \sigma^2 \mathbf{b}^H[m]\mathbf{S}[m]\mathbf{S}[m]\mathbf{b}[m]} = \frac{\frac{1}{4}P_t \min_{i,j} \mathbf{b}^H[m]\mathbf{D}_{i,j}\mathbf{b}[m]}{\delta^2 \mathbf{b}^H[m]\mathbf{b}[m] + \sigma^2 \mathbf{b}^H[m]\mathbf{S}[m]\mathbf{S}[m]\mathbf{b}[m]}, \quad (7)$$

$$\mathbf{D}_{i,j} = \mathbf{S}[m]\mathbf{H}\left(\mathbf{q}_i[m] - \mathbf{q}_j[m]\right)\left(\mathbf{q}_i[m] - \mathbf{q}_j[m]\right)^H \mathbf{H}^H \mathbf{S}^H[m]. \quad (8)$$

Since only the closest two constellation points are considered, the probability of symbol error in mth symbol interval is upper bounded by [15]

$$p_e \leq Q\left(\sqrt{2\mathrm{SNR}_{\mathrm{mod}}[m]}\right). \quad (9)$$

The harvested energy from all EHs is guided to the common energy storage. The input signal of each energy harvester is

$$y_k[m] = \sqrt{P_t}\mathbf{e}_k^T\left(\mathbf{H}\mathbf{a}[m] + \mathbf{w}[m]\right)\sqrt{1-\rho_k}, \quad (10)$$

where $\mathbf{e}_k$ is a column vector with all-zero elements except for a single '1' at kth position. The total instantaneous harvested energy is obtained using (10) as

$$E_{\mathrm{harv}}[m] = \eta T \sum_k |y_k[m]|^2 \approx \eta T P_t \mathbf{a}^H[m]\mathbf{H}^H\left(\mathbf{I} - \mathbf{S}[m]\mathbf{S}[m]\right)\mathbf{H}\mathbf{a}[m], \quad (11)$$

where η is the energy harvesting rate. In this work, we assume a linear energy harvesting model with $\eta = 0.5$. The impact of the well-known non-linear behavior of the energy harvesting circuits (cf. [16]) on the optimization performance is beyond the scope of this work.

III. Harvested Power Maximization

In this work, we focus on the harvested energy under the constraint of ultrareliability in RMA. Note, that we do not address the typical trade-off between information and power transfer in terms of rate-energy region, cf. [17]. As argued in [8], in order to guarantee ultrareliable communication, the signal quality needs to be permanently very high, which renders the rate-energy region analysis irrelevant.

In order to jointly optimize the power splitting factors and the beamforming coefficients, we formulate the following optimization problem:

$$\begin{aligned} \max_{\substack{\rho_k, b_k, \\ 1\leq k\leq N_{\mathrm{ant}}}} \quad & \mathcal{E}\{E_{\mathrm{harv}}[m]\}, \quad (12) \\ \text{s.t.:} \quad & \mathrm{C1})\ p_e \leq p_{\max}, \\ & \mathrm{C2})\ 0 < \rho_k \leq 1,\ 1 \leq k \leq K, \\ & \mathrm{C3})\ \min_{i,j} d_{i,j}[m] \text{ unknown}. \end{aligned}$$

Here, we introduce the ultrareliability constraint C1) by choosing a very low target symbol error rate $p_{\max}$. Furthermore, the constraint C3) is introduced in order to account for the fact that the symbol constellation and the corresponding minimum Euclidean distance between the symbols are unknown before the symbol detection.

Similarly to [8], this problem requires a prediction of the minimum distance between the constellation points.

A. Constellation prediction

We consider the following options for predicting the minimum distance between symbols of the unknown constellation:

- *Static beamforming*: The optimization is carried out only once and the system parameters are assumed to be constant for all symbol intervals m. In this case, all possible symbol combinations need to be taken into account. Hence, this option leads to the performance lower bound as explained in [8], since the number of points is maximal while the average received energy is the same for all valid solutions. The corresponding minimum distance between the symbol points is typically very small, such that energy harvesting is rarely possible;
- *Genie-Aided Prediction*: In case of dynamic beamforming, the unknown parameters need to be optimized and updated in every symbol interval. Since the exact symbol constellation is unknown before the detection of the respective symbol, the constellation needs to be predicted. Here, a perfect (genie-aided) prediction corresponds to the performance upper bound. For this, we assume that the relay knows exactly, which nodes are active, such that only the valid symbol points are considered;
- *State Prediction*: The prediction is carried out using the method proposed in [8], where the state of each node (i.e. active or not) is predicted based on the previous observations of the received signal. The respective most probable receive symbols are collected and form the joint constellation. So far, this method has shown a substantial performance gain compared to the lower bound with $K = 1$, especially in case of a large number of nodes.

Assuming one of these options, $\min_{i,j} d_{i,j}[m]$ can be predicted, such that the constraint C3) is relaxed. The resulting relaxed optimization problem is solved in the following.

B. Optimization problem with known constellation

By relaxing constraint C3) in (12), we remove the uncertainty related to the RMA. The resulting problem is non-linear and non-convex, as can be deduced from (7), such that the well-known methods of convex optimization [18] are not applicable here and no analytic solution can be found. However, we can solve the relaxed problem by splitting it in two subproblems, which have a much lower complexity and can be solved alternatingly. In general, the idea of this approach is to reduce the power splitting factor by maximizing the Euclidean distance between all points of the joint constellation, since less signal power would be required for the symbol detection.

Note, that for the clarity of exposition, we omit the symbol interval index m in the following.

At first, we rewrite (11) as

$$E_{\mathrm{harv}} = \eta T P_t \mathcal{E}\{\mathbf{a}^H\mathbf{H}^H\mathbf{H}\mathbf{a}\} - \mathbf{s}^H\mathbf{Y}\mathbf{s}, \quad (13)$$

where $\mathbf{s} = vec(\sqrt{\rho}, K)$ and $\mathbf{Y} = \eta T P_t \mathcal{E}\{\mathbf{H}\mathbf{a}\mathbf{a}^H\mathbf{H}^H\}$.

Then, constraint C1) can be reformulated using (7) and (9):

$$\mathbf{b}^H\mathbf{D}_{i,j}\mathbf{b} \geq \left(\delta^2\mathbf{b}^H\mathbf{b} + \sigma^2\mathbf{b}^H\mathbf{S}^H\mathbf{S}\mathbf{b}\right)\frac{2\left(Q^{-1}\left(p_{\max}\right)\right)^2}{P_t},\ \forall i,j. \quad (14)$$

This constraint can be further expressed as a standard quadratic form with respect to $\mathbf{b}$

$$\mathbf{b}^H \mathbf{T}_{i,j} \mathbf{b} \leq 0, \; \forall i, j, \tag{15}$$

$$\mathbf{T}_{i,j} = \left(\delta^2 \mathbf{I} + \sigma^2 \mathbf{S}^H \mathbf{S} \right) \frac{2 \left(Q^{-1} \left(p_{\max} \right) \right)^2}{P_t} - \mathbf{D}_{i,j}. \tag{16}$$

On the other hand, this constraint can be expressed with respect to $\mathbf{s}$ as well. For this, we first reformulated the distance function $d_{i,j}$ using (6) as

$$d_{i,j} = \sqrt{P_t} \left| \mathbf{b}^H \mathbf{Q}_{i,j} \mathbf{s} \right| \tag{17}$$

with the diagonal matrix $\mathbf{Q}_{i,j} = diag(\mathbf{H} \left(\mathbf{q}_i - \mathbf{q}_j \right))$. After few reformulation steps, we obtain for the constraint C1)

$$\mathbf{s}^H \mathbf{K}_{i,j} \mathbf{s} \leq D, \; \forall i, j, \tag{18}$$

where we introduce $\mathbf{B} = diag(\mathbf{b})^H diag(\mathbf{b})$ in order to obtain

$$\mathbf{K}_{i,j} = \frac{2\sigma^2}{P_t} \left(Q^{-1} \left(p_{\max} \right) \right)^2 \mathbf{B} - \mathbf{Q}_{i,j} \mathbf{b} \mathbf{b}^H \mathbf{Q}_{i,j}, \tag{19}$$

$$D = -\frac{2\delta^2}{P_t} \left(Q^{-1} \left(p_{\max} \right) \right)^2 \mathbf{b}^H \mathbf{b}. \tag{20}$$

Using (13), (15), and (18), we can express the relaxed optimization problem as

$$\begin{aligned} &\min_{\mathbf{s},\, \mathbf{b}} \mathbf{s}^H \mathbf{Y} \mathbf{s}, \qquad (21) \\ &\text{s.t.:} \quad \text{C1a)} \; \mathbf{b}^H \mathbf{T}_{i,j} \mathbf{b} \leq 0, \; \forall i, j, \;\; \text{C1b)} \; \mathbf{s}^H \mathbf{K}_{i,j} \mathbf{s} \leq D, \; \forall i, j, \\ &\qquad \text{C2)} \; 0 \prec \mathbf{s} \preceq 1. \end{aligned}$$

Here, the two constraints C1a) and C1b) are equivalent representations of the original constraint C1) of problem (12). Apparently, the two matrices $\mathbf{T}_{i,j}$ and $\mathbf{K}_{i,j}$ depend non-linearly on $\mathbf{s}$ and $\mathbf{b}$, respectively, which makes (21) a non-linear program. However, we can split this problem in two sub-problems, which are quadratically constrained quadratic programs (QCQPs).

The first sub-problem is the maximization of the harvested energy:

$$\begin{aligned} &\min_{\mathbf{s}} \mathbf{s}^H \mathbf{Y} \mathbf{s}, \qquad (22) \\ &\text{s.t.:} \quad \text{C1)} \; \mathbf{s}^H \mathbf{K}_{i,j} \mathbf{s} \leq D, \; \forall i, j, \\ &\qquad \text{C2)} \; 0 \prec \mathbf{s} \preceq 1. \end{aligned}$$

We assume that the beamforming coefficients are fixed and known, e.g. from the previous calculation. Hence, matrix $\mathbf{K}_{i,j}$ is considered to be constant in this sub-problem.

As discussed earlier, we would like to maximize the minimum distance between all points of the joint constellation in order to reduce the required signal power for the symbol detection and thus increase the harvested energy. Note, that the maximization of the minimum distance corresponds to the minimization of $\mathbf{b}^H \mathbf{T}_{i,j} \mathbf{b}$, $\forall i, j$ according to the derivations above and the definition of matrix $\mathbf{T}_{i,j}$ in (16). Hence, we introduce an auxiliary variable τ, which corresponds to the maximum $\mathbf{b}^H \mathbf{T}_{i,j} \mathbf{b}$ and formulate the second sub-problem as

$$\begin{aligned} &\min_{\mathbf{b}, \tau} \tau, \qquad (23) \\ &\text{s.t.:} \quad \text{C1)} \; \mathbf{b}^H \mathbf{T}_{i,j} \mathbf{b} \leq \tau \; \forall i, j. \end{aligned}$$

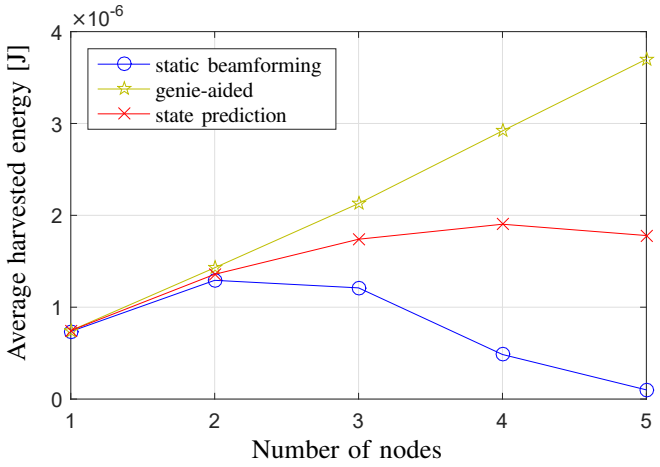

Fig. 3. Average harvested energy per second with a variable number of nodes.

Here, we assume that the power splitting factors are fixed and known from the previous calculation, which makes matrix $\mathbf{T}_{i,j}$ constant for this sub-problem.

Both sub-problems are non-convex QCQPs. The non-convexity is due to the indefinite matrices $\mathbf{K}_{i,j}$ and $\mathbf{T}_{i,j}$ $\forall i, j$. Nevertheless, we solve these problems using a close-to-optimum method of Successive Convex Approximation (SCA) called Feasible Point Pursuit (FPP), cf. [19]. In each iteration of our alternating approach, we solve sub-problems (22) and (23) subsequently. For this, the respective optimized parameters of one sub-problem are assumed fixed in the other sub-problem. The optimization starts by solving the second sub-problem (beamforming). For this, we assume fixed power splitting factors $\rho_k = 1, \forall k$, i.e. all energy harvesting modules are disabled. In total, the algorithm is run for J iterations, where $J = 5$ is usually sufficient for convergence.

IV. Numerical Results

In our simulations, we assume that the nodes are randomly deployed in the distance between 5 m and 10 m around the relay according to Fig. 1. Also, an equal transmit power $P_t = 20$ dBm for all nodes, a bandwidth of 1 kHz, and a carrier frequency of 900 MHz are assumed. For the signal propagation, a Rician flat fading channel with the line-of-sight factor 3, a path loss exponent 2, and additive white Gaussian noise with respective variance $\sigma^2 = -110$ dBm and $\delta^2 = -70$ dBm are used. For the energy conversion efficiency, we set $\eta = 0.5$. Each node transmits packets of equal length $L_n = 20, \forall n$ with equal probability $p_n = p, \forall n$. Furthermore, we set the target bit error rate $p_{\max} = 10^{-6}$. The results are averaged over 1000 scenarios for each simulation point. In each scenario, a received sequence of 500 symbols is considered.

We start with the evaluation of the average harvested energy for $K = 2$ and a variable number of nodes N, see Fig. 3. We observe that the harvested energy using the genie-aided predictor increases with increasing number of nodes, since the received signal variance depends on the number of simultaneous transmissions. On the other hand, the static beamforming solution shows a maximum of harvested energy for $N = 2$ followed by a performance degradation

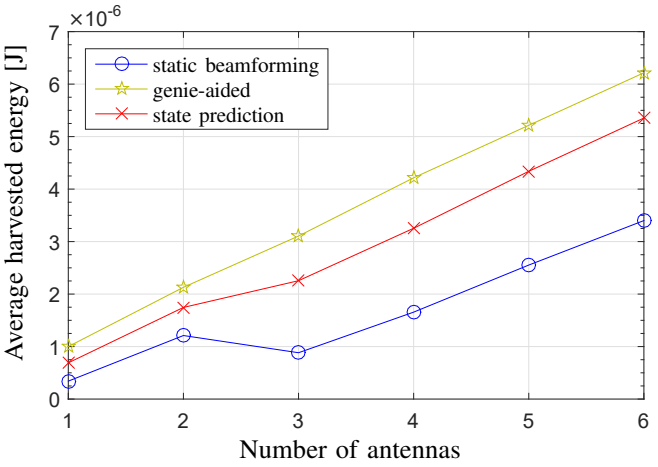

Fig. 4. Average harvested energy per second with a variable number of receive antennas.

for $N \geq 3$. This degradation results from the increased number of symbols in the joint constellation, which leads to a smaller minimum distance between the individual symbols. In addition, a performance degradation is observed with the state prediction method as well. However, this degradation occurs with a larger number of nodes, such that a performance gain results compared to the static beamforming. A similar behavior has been noticed in [8] for $K = 1$.

In addition, we show the results for $N = 3$ and a variable number of receive antennas K, see Fig. 4. Obviously, the performance of genie-aided and state prediction methods increases with increasing number of antennas, since more energy harvesters are utilized. Surprisingly, the average harvested energy using static beamforming method has at first a maximum for $K = 2$ followed by a decrease for $K = 3$ and then a linear increase for $K \geq 4$. The decrease from $K = 2$ to $K = 3$ indicates the suboptimality of the proposed optimization method. In fact, the Lagrangian for the optimization problem has many local optima due to the non-convexity of the constraints. Their number increases with the number of antennas due to the increased spatial diversity. Furthermore, each constraint contributes to the Lagrangian with an additional set of local optima. Since the static beamforming method takes into account the maximum number of constellation points and correspondingly the maximum number of constraints, it is likely for this method to converge to a local optimum, which typically shows a very poor performance. Similarly, a deviation from the linear curve is observed with the state prediction method for $K = 3$. However, this effect is less pronounced, since the number of constraints is significantly lower than with the static beamforming method. For $K \geq 4$, we observe a difference of ≈ 2.7 μJ between the static beamforming and the genie-aided prediction, whereas the difference between the state prediction and the genie-aided prediction is only ≈ 1 μJ.

V. Conclusion

In this paper, we analyzed a random access based ultrareliable SWIPT with application to a relay-based uplink with multiple receive antennas. The design implies a (non-convex) joint optimization of the power splitting factor per antenna and the beamforming coefficients for the information stream as well as a prediction of the symbol constellation in each symbol interval. At first, various options with respect to the constellation prediction have been addressed. Then, a suboptimal solution for the optimization problem has been proposed by splitting it in two sub-problems and solving them alternatingly. We observe a performance degradation using the static beamforming and the state prediction method for relatively large numbers of nodes. On the other hand, the average harvested energy using the state prediction method increases monotonically with increasing number of antennas, which motivates the application of massive MIMO for this scenario.

References

[1] L. Atzori, A. Iera, and G. Morabito, "The Internet of Things: A survey," *Computer networks*, vol. 54, no. 15, pp. 2787–2805, 2010.

[2] Y. Saito, Y. Kishiyama, A. Benjebbour, T. Nakamura, A. Li, and K. Higuchi, "Non-orthogonal multiple access (NOMA) for cellular future radio access," in *Vehicular Technology Conference (VTC Spring), 2013 IEEE 77th*. IEEE, 2013, pp. 1–5.

[3] S. Kisseleff, J. Kneissl, G. Kilian, and W. Gerstacker, "Optimal MAP Detection in Presence of Burst Interference for Low Power Wide Area Networks," in *Proceedings of IEEE Globecom*, 2018, pp. 1–5.

[4] G. Durisi, T. Koch, and P. Popovski, "Toward Massive, Ultrareliable, and Low-Latency Wireless Communication With Short Packets," *Proceedings of the IEEE*, vol. 104, no. 9, pp. 1711–1726, Sept 2016.

[5] C. She, C. Yang, and T. Quek, "Radio Resource Management for Ultra-Reliable and Low-Latency Communications," *IEEE Communications Magazine*, vol. 55, no. 6, pp. 72–78, June 2017.

[6] Y. Hu, M. Gursoy, and A. Schmeink, "Relaying-Enabled Ultra-Reliable Low-Latency Communications in 5G," *IEEE Network*, vol. 32, no. 2, pp. 62–68, March 2018.

[7] T. Vu, C. Liu, M. Bennis, M. Debbah, M. Latva-aho, and C. Hong, "Ultra-Reliable and Low Latency Communication in mmWave-Enabled Massive MIMO Networks," *IEEE Communications Letters*, vol. 21, no. 9, pp. 2041–2044, Sept 2017.

[8] S. Kisseleff, S. Chatzinotas, and B. Ottersten, "Ultrareliable SWIPT using Unscheduled Short Packet Transmissions," *accepted for presentation at IEEE ICC 2019*.

[9] T. Perera, D. Jayakody, S. Sharma, S. Chatzinotas, and J. Li, "Simultaneous wireless information and power transfer (SWIPT): Recent advances and future challenges," *IEEE Communications Surveys & Tutorials*, vol. 20, no. 1, pp. 264–302, 2017.

[10] A. Kariminezhad, S. Gherekhloo, and A. Sezgin, "Optimal power splitting for simultaneous information detection and energy harvesting," *IEEE Signal Processing Letters*, vol. 24, no. 7, pp. 963–967, July 2017.

[11] A. Kariminezhad and A. Sezgin, "Towards optimal energy harvesting receiver design in mimo systems," *arXiv preprint arXiv:1711.02030*, 2017.

[12] R. Zhang and C. Ho, "MIMO broadcasting for simultaneous wireless information and power transfer," *IEEE Transactions on Wireless Communications*, vol. 12, no. 5, pp. 1989–2001, 2013.

[13] L. Liu, R. Zhang, and K.-C. Chua, "Wireless information and power transfer: A dynamic power splitting approach," *IEEE Transactions on Communications*, vol. 61, no. 9, pp. 3990–4001, 2013.

[14] S. Verdu, *Multiuser Detection*. Cambridge University Press, 1998.

[15] A. Goldsmith, *Wireless Communications*. Cambridge University Press, 2005.

[16] E. Boshkovska, D. Ng, N. Zlatanov, and R. Schober, "Practical non-linear energy harvesting model and resource allocation for SWIPT systems," *IEEE Communications Letters*, vol. 19, no. 12, pp. 2082–2085, 2015.

[17] Q. Shi, L. Liu, W. Xu, and R. Zhang, "Joint Transmit Beamforming and Receive Power Splitting for MISO SWIPT Systems," *IEEE Transactions on Wireless Communications*, vol. 13, no. 6, pp. 3269–3280, June 2014.

[18] S. Boyd and L. Vandenberghe, *Convex Optimization*. Cambridge University Press, 2004.

[19] O. Mehanna, K. Huang, B. Gopalakrishnan, A. Konar, and N. Sidiropoulos, "Feasible point pursuit and successive approximation of non-convex QCQPs," *IEEE Signal Processing Letters*, vol. 22, no. 7, pp. 804–808, 2015.